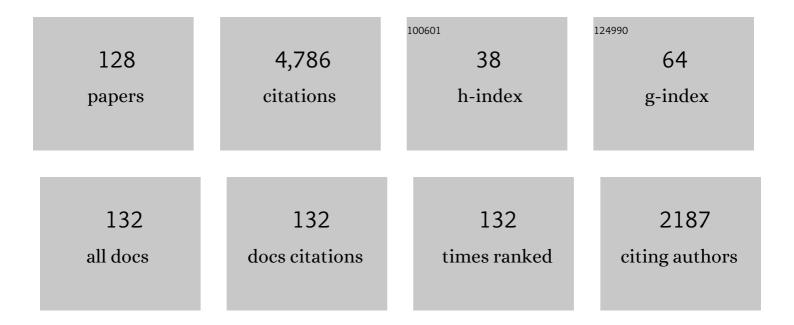
List of Publications by Year in descending order

Source: https://exaly.com/author-pdf/3374443/publications.pdf Version: 2024-02-01



#	Article	IF	CITATIONS
1	The Biomarkers in the Mesoproterozoic Organicâ€rich Rocks of North China Craton: Implication for the Precursor and Preservation of Organism in the Prokaryotic Realm. Acta Geologica Sinica, 2022, 96, 293-308.	0.8	3
2	Application of Cd as a paleo-environment indicator. Palaeogeography, Palaeoclimatology, Palaeoecology, 2022, 585, 110749.	1.0	4
3	Multielement Imaging Reveals the Diagenetic Features and Varied Water Redox Conditions of a Lacustrine Dolomite Nodule. Geofluids, 2022, 2022, 1-20.	0.3	2
4	New chronological and paleontological evidence for Paleoproterozoic eukaryote distribution and stratigraphic correlation between the Yanliao and Xiong'er basins, North China Craton. Precambrian Research, 2022, 371, 106577.	1.2	10
5	Mesoproterozoic marine biological carbon pump: Source, degradation, and enrichment of organic matter. Chinese Science Bulletin, 2022, 67, 1624-1643.	0.4	12
6	The effect of biodegradation on bound aromatic hydrocarbons released from intermediate-temperature gold-tube pyrolysis of severely biodegraded Athabasca bitumen. Journal of Analytical and Applied Pyrolysis, 2022, 163, 105497.	2.6	1
7	Effects of inorganic sulfur species on hydrocarbon conversion and 34S isotope fractionation during thermal maturation of Type II kerogen. Organic Geochemistry, 2022, 168, 104420.	0.9	1
8	Did high temperature rather than low O2 hinder the evolution of eukaryotes in the Precambrian?. Precambrian Research, 2022, 378, 106755.	1.2	4
9	Sedimentary Environments of Cambrian–Ordovician Source Rocks and Ultraâ€deep Petroleum Accumulation in the Tarim Basin. Acta Geologica Sinica, 2022, 96, 1259-1276.	0.8	4
10	Pyrolysis of 1-methylnaphthalene involving water: Effects of Fe-bearing minerals on the generation, C and H isotope fractionation of methane from H2O-hydrocarbon reaction. Organic Geochemistry, 2021, 153, 104151.	0.9	7
11	Using cyclostratigraphic evidence to define the unconformity caused by the Mesoproterozoic Qinyu Uplift in the North China Craton. Journal of Asian Earth Sciences, 2021, 206, 104608.	1.0	16
12	Molecular and carbon isotopic evidence of pigments indicating a dynamic oceanic chemocline 1.4 billion years ago in northern China. Organic Geochemistry, 2021, 154, 104207.	0.9	4
13	Eukaryotic red and green algae populated the tropical ocean 1400 million years ago. Precambrian Research, 2021, 357, 106166.	1.2	25
14	Petrographic carbon in ancient sediments constrains Proterozoic Era atmospheric oxygen levels. Proceedings of the National Academy of Sciences of the United States of America, 2021, 118, .	3.3	30
15	Recognizing the pathways of microbial methanogenesis through methane isotopologues in the subsurface biosphere. Earth and Planetary Science Letters, 2021, 566, 116960.	1.8	8
16	The environmental context of carbonaceous compressions and implications for organism preservation 1.40ÂGa and 0.63ÂGa. Palaeogeography, Palaeoclimatology, Palaeoecology, 2021, 573, 110449.	1.0	8
17	Decoupled Cr, Mo, and U records of the Hongshuizhuang Formation, North China: Constraints on the Mesoproterozoic ocean redox. Marine and Petroleum Geology, 2021, 132, 105243.	1.5	4
18	Evolution of the 1.8–1.6ÂGa Yanliao and Xiong'er basins, north China Craton. Precambrian Research, 2021, 365, 106383.	1.2	12

#	Article	IF	CITATIONS
19	Quantitative measurement of interaction strength between kaolinite and different oil fractions via atomic force microscopy: Implications for clay-controlled oil mobility. Marine and Petroleum Geology, 2021, 133, 105296.	1.5	3
20	The Mesoproterozoic Oxygenation Event. Science China Earth Sciences, 2021, 64, 2043-2068.	2.3	20
21	Multi-Element Imaging of a 1.4 Ga Authigenic Siderite Crystal. Minerals (Basel, Switzerland), 2021, 11, 1395.	0.8	4
22	The effect of biodegradation on bound biomarkers released from intermediate-temperature gold-tube pyrolysis of severely biodegraded Athabasca bitumen. Fuel, 2020, 263, 116669.	3.4	14
23	Hydrothermal experiments involving methane and sulfate: Insights into carbon isotope fractionation of methane during thermochemical sulfate reduction. Organic Geochemistry, 2020, 149, 104101.	0.9	7
24	Tracking the evolution of seawater Mo isotopes through the Ediacaran–Cambrian transition. Precambrian Research, 2020, 350, 105929.	1.2	13
25	Hydrocarbon generation from bacterial biomass in ca. 1320 million years ago. IOP Conference Series: Earth and Environmental Science, 2020, 600, 012032.	0.2	3
26	An astronomically calibrated stratigraphy of the Mesoproterozoic Hongshuizhuang Formation, North China: Implications for pre-Phanerozoic changes in Milankovitch orbital parameters. Journal of Asian Earth Sciences, 2020, 199, 104408.	1.0	8
27	The modern phosphorus cycle informs interpretations of Mesoproterozoic Era phosphorus dynamics. Earth-Science Reviews, 2020, 208, 103267.	4.0	36
28	Carbon and hydrogen isotope fractionation for methane from non-isothermal pyrolysis of oil in anhydrous and hydrothermal conditions. Energy Exploration and Exploitation, 2019, 37, 1558-1576.	1.1	11
29	Experimental and theoretical studies on kinetics for thermochemical sulfate reduction of oil, C2–5 and methane. Journal of Analytical and Applied Pyrolysis, 2019, 139, 59-72.	2.6	25
30	Paleoenvironmental proxies and what the Xiamaling Formation tells us about the midâ€Proterozoic ocean. Geobiology, 2019, 17, 225-246.	1.1	41
31	Hydrocarbon generation characteristics and exploration prospects of Proterozoic source rocks in China. Science China Earth Sciences, 2019, 62, 909-934.	2.3	41
32	Origin of conventional and shale gas in Sinian–lower Paleozoic strata in the Sichuan Basin: Relayed gas generation from liquid hydrocarbon cracking. AAPG Bulletin, 2019, 103, 1265-1296.	0.7	18
33	Gas generation potential and processes of Athabasca oil sand bitumen from gold tube pyrolysis experiments. Fuel, 2019, 239, 804-813.	3.4	13
34	A Mesoproterozoic iron formation. Proceedings of the National Academy of Sciences of the United States of America, 2018, 115, E3895-E3904.	3.3	61
35	Pyrolysis involving n -hexadecane, water and minerals: Insight into the mechanisms and isotope fractionation for water-hydrocarbon reaction. Journal of Analytical and Applied Pyrolysis, 2018, 130, 198-208.	2.6	22
36	Petroleum geological conditions and exploration importance of Proterozoic to Cambrian in China. Petroleum Exploration and Development, 2018, 45, 1-14.	3.0	67

#	Article	IF	CITATIONS
37	Marine redox variations during the Ediacaran–Cambrian transition on the Yangtze Platform, South China. Geological Journal, 2018, 53, 58-79.	0.6	20
38	Unique chemical and isotopic characteristics and origins of natural gases in the Paleozoic marine formations in the Sichuan Basin, SW China: Isotope fractionation of deep and high mature carbonate reservoir gases. Marine and Petroleum Geology, 2018, 89, 68-82.	1.5	51
39	The upper thermal maturity limit of primary gas generated from marine organic matters. Marine and Petroleum Geology, 2018, 89, 120-129.	1.5	12
40	The evolution of chemical groups and isotopic fractionation at different maturation stages during lignite pyrolysis. Fuel, 2018, 211, 492-506.	3.4	37
41	Equilibrium and non-equilibrium controls on the abundances of clumped isotopologues of methane during thermogenic formation in laboratory experiments: Implications for the chemistry of pyrolysis and the origins of natural gases. Geochimica Et Cosmochimica Acta, 2018, 223, 159-174.	1.6	32
42	The aerobic diagenesis of Mesoproterozoic organic matter. Scientific Reports, 2018, 8, 13324.	1.6	12
43	Contrasting Mo–U enrichments of the basal Datangpo Formation in South China: Implications for the Cryogenian interglacial ocean redox. Precambrian Research, 2018, 315, 66-74.	1.2	33
44	Highly fractionated chromium isotopes in Mesoproterozoic-aged shales and atmospheric oxygen. Nature Communications, 2018, 9, 2871.	5.8	130
45	Significance of source rock heterogeneities: A case study of Mesoproterozoic Xiamaling Formation shale in North China. Petroleum Exploration and Development, 2017, 44, 32-39.	3.0	30
46	Oxygen, climate and the chemical evolution of a 1400 million year old tropical marine setting. Numerische Mathematik, 2017, 317, 861-900.	0.7	67
47	Effects of U-ore on the chemical and isotopic composition of products of hydrous pyrolysis of organic matter. Petroleum Science, 2017, 14, 315-329.	2.4	9
48	The oxic degradation of sedimentary organic matter 1400 Ma constrains atmospheric oxygen levels. Biogeosciences, 2017, 14, 2133-2149.	1.3	43
49	Remarkable Preservation of Microfossils and Biofilms in Mesoproterozoic Silicified Bitumen Concretions from Northern China. Geofluids, 2017, 2017, 1-12.	0.3	4
50	New Insight into the Kinetics of Deep Liquid Hydrocarbon Cracking and Its Significance. Geofluids, 2017, 2017, 1-11.	0.3	7
51	Geofluids in Deep Sedimentary Basins and Their Significance for Petroleum Accumulation. Geofluids, 2017, 2017, 1-4.	0.3	3
52	Reply to Planavsky et al.: Strong evidence for high atmospheric oxygen levels 1,400 million years ago. Proceedings of the National Academy of Sciences of the United States of America, 2016, 113, E2552-3.	3.3	17
53	Microbial consortia controlling biogenic gas formation in the Qaidam Basin of western China. Journal of Geophysical Research G: Biogeosciences, 2016, 121, 2296-2309.	1.3	5
54	Palaeozoic oil–source correlation in the Tarim Basin, NW China: A review. Organic Geochemistry, 2016, 94, 32-46.	0.9	110

#	Article	IF	CITATIONS
55	Sufficient oxygen for animal respiration 1,400 million years ago. Proceedings of the National Academy of Sciences of the United States of America, 2016, 113, 1731-1736.	3.3	259
56	Upper thermal maturity limit for gas generation from humic coal. International Journal of Coal Geology, 2015, 152, 123-131.	1.9	11
57	Origin of diamondoid and sulphur compounds in the Tazhong Ordovician condensate, Tarim Basin, China: Implications for hydrocarbon exploration in deep-buried strata. Marine and Petroleum Geology, 2015, 62, 14-27.	1.5	31
58	Geochemistry of Paleozoic marine petroleum from the Tarim Basin, NW China: Part 5. Effect of maturation, TSR and mixing on the occurrence and distribution of alkyldibenzothiophenes. Organic Geochemistry, 2015, 86, 5-18.	0.9	40
59	Orbital forcing of climate 1.4 billion years ago. Proceedings of the National Academy of Sciences of the United States of America, 2015, 112, E1406-13.	3.3	110
60	Ultra-deep liquid hydrocarbon exploration potential in cratonic region of the Tarim Basin inferred from gas condensate genesis. Fuel, 2015, 160, 583-595.	3.4	46
61	Genetic origin of sour gas condensates in the Paleozoic dolomite reservoirs of the Tazhong Uplift, Tarim Basin. Marine and Petroleum Geology, 2015, 68, 107-119.	1.5	30
62	Geochemistry of alkylbenzenes in the Paleozoic oils from the Tarim Basin, NW China. Organic Geochemistry, 2014, 77, 126-139.	0.9	31
63	The speciation of aqueous sulfate and its implication on the initiation mechanisms of TSR at different temperatures. Applied Geochemistry, 2014, 43, 121-131.	1.4	27
64	Biogeochemical identification of the Quaternary biogenic gas source rock in the Sanhu Depression, Qaidam Basin. Organic Geochemistry, 2014, 73, 101-108.	0.9	18
65	Geochemistry of Paleozoic marine oils from the Tarim Basin, NW China. Part 4: Paleobiodegradation and oil charge mixing. Organic Geochemistry, 2014, 67, 41-57.	0.9	81
66	Secondary accumulation of hydrocarbons in Carboniferous reservoirs in the northern Tarim Basin, China. Journal of Petroleum Science and Engineering, 2013, 102, 10-26.	2.1	32
67	Charging time of tight gas in the Upper Paleozoic of the Ordos Basin, central China. Organic Geochemistry, 2013, 64, 38-46.	0.9	41
68	Controls on biogenic gas formation in the Qaidam Basin, northwestern China. Chemical Geology, 2013, 335, 36-47.	1.4	26
69	Occurrence of heavy carbon dioxide of organic origin: Evidence from confined dry pyrolysis of coal. Chemical Geology, 2013, 358, 54-60.	1.4	12
70	Timing of biogenic gas formation in the eastern Qaidam Basin, NW China. Chemical Geology, 2013, 352, 70-80.	1.4	25
71	Alteration and multi-stage accumulation of oil and gas in the Ordovician of the Tabei Uplift, Tarim Basin, NW China: Implications for genetic origin of the diverse hydrocarbons. Marine and Petroleum Geology, 2013, 46, 234-250.	1.5	89
72	Synthesis of hydrocarbon gases from four different carbon sources and hydrogen gas using a gold-tube system by Fischer–Tropsch method. Chemical Geology, 2013, 349-350, 27-35.	1.4	51

#	Article	IF	CITATIONS
73	Stable hydrogen and carbon isotopic ratios of coal-derived and oil-derived gases: A case study in the Tarim basin, NW China. International Journal of Coal Geology, 2013, 116-117, 302-313.	1.9	33
74	Identification and distribution of marine hydrocarbon source rocks in the Ordovician and Cambrian of the Tarim Basin. Petroleum Exploration and Development, 2012, 39, 305-314.	3.0	37
75	Adjustment and alteration of hydrocarbon reservoirs during the Late Himalayan Period, Tarim Basin, NW China. Petroleum Exploration and Development, 2012, 39, 712-724.	3.0	28
76	The occurrence of ultra-deep heavy oils in the Tabei Uplift of the Tarim Basin, NW China. Organic Geochemistry, 2012, 52, 88-102.	0.9	92
77	Molecular carbon isotope variations in core samples taken at the Permian–Triassic boundary layers in southern China. International Journal of Earth Sciences, 2012, 101, 1397-1406.	0.9	0
78	Gas genetic type and origin of hydrogen sulfide in the Zhongba gas field of the western Sichuan Basin, China. Applied Geochemistry, 2011, 26, 1261-1273.	1.4	81
79	Fundamental studies on kinetic isotope effect (KIE) of hydrogen isotope fractionation in natural gas systems. Geochimica Et Cosmochimica Acta, 2011, 75, 2696-2707.	1.6	81
80	Geochemical evidence for coal-derived hydrocarbons and their charge history in the Dabei Gas Field, Kuqa Thrust Belt, Tarim Basin, NW China. Marine and Petroleum Geology, 2011, 28, 1364-1375.	1.5	68
81	A novel method for isolation of diamondoids from crude oils for compound-specific isotope analysis. Organic Geochemistry, 2011, 42, 566-571.	0.9	13
82	Geochemical characterization of secondary microbial gas occurrence in the Songliao Basin, NE China. Organic Geochemistry, 2011, 42, 781-790.	0.9	22
83	Geochemistry of Palaeozoic marine petroleum from the Tarim Basin, NW China: Part 3. Thermal cracking of liquid hydrocarbons and gas washing as the major mechanisms for deep gas condensate accumulations. Organic Geochemistry, 2011, 42, 1394-1410.	0.9	114
84	Mechanism of catalytic hydropyrolysis of sedimentary organic matter with MoS2. Petroleum Science, 2011, 8, 134-142.	2.4	11
85	Comparison of geochemical parameters derived from comprehensive two-dimensional gas chromatography with time-of-flight mass spectrometry and conventional gas chromatography-mass spectrometry. Science China Earth Sciences, 2011, 54, 1892-1901.	2.3	9
86	Geochemistry of coal-measure source rocks and natural gases in deep formations in Songliao Basin, NE China. International Journal of Coal Geology, 2010, 84, 276-285.	1.9	34
87	Geochemical evidence for strong ongoing methanogenesis in Sanhu region of Qaidam Basin. Science China Earth Sciences, 2010, 53, 84-90.	2.3	8
88	Identification of petroleum aromatic fraction by comprehensive two-dimensional gas chromatography with time-of-flight mass spectrometry. Science Bulletin, 2010, 55, 2039-2045.	1.7	16
89	Induced H2S formation during steam injection recovery process of heavy oil from the Liaohe Basin, NE China. Journal of Petroleum Science and Engineering, 2010, 71, 30-36.	2.1	31
90	The effects of calcite and montmorillonite on oil cracking in confined pyrolysis experiments. Organic Geochemistry, 2010, 41, 611-626.	0.9	127

SHUICHANG ZHANG

#	Article	IF	CITATIONS
91	Relationship between the later strong gas-charging and the improvement of the reservoir capacity in deep Ordovician carbonate reservoir in Tazhong area, Tarim Basin. Science Bulletin, 2009, 54, 3076-3089.	1.7	41
92	TSR promotes the formation of oil-cracking gases: Evidence from simulation experiments. Science in China Series D: Earth Sciences, 2008, 51, 451-455.	0.9	20
93	The components and carbon isotope of the gases in inclusions in reservoir layers of Upper Paleozoic gas pools in the Ordos Basin, China. Science in China Series D: Earth Sciences, 2008, 51, 115-121.	0.9	6
94	Natural gas origins of large and medium-scale gas fields in China sedimentary basins. Science in China Series D: Earth Sciences, 2008, 51, 1-13.	0.9	44
95	Detection of 2-thiaadamantanes in the oil from Well TZ-83 in Tarim Basin and its geological implication. Science Bulletin, 2008, 53, 396-401.	1.7	32
96	Biogenic gas systems in eastern Qaidam Basin. Marine and Petroleum Geology, 2008, 25, 344-356.	1.5	37
97	Petroleum geology of the Puguang sour gas field in the Sichuan Basin, SW China. Marine and Petroleum Geology, 2008, 25, 357-370.	1.5	187
98	Oil–source correlation in Tertiary deltaic petroleum systems: A comparative study of the Beaufort–Mackenzie Basin in Canada and the Pearl River Mouth Basin in China. Organic Geochemistry, 2008, 39, 1170-1175.	0.9	19
99	Ruthenium-ion-catalyzed oxidation of asphaltenes of heavy oils in Lunnan and Tahe oilfields in Tarim Basin, NW China. Organic Geochemistry, 2008, 39, 1502-1511.	0.9	37
100	Diamondoid hydrocarbons as a molecular proxy for thermal maturity and oil cracking: Geochemical models from hydrous pyrolysis. Organic Geochemistry, 2007, 38, 227-249.	0.9	124
101	The Xiamaling oil shale generated through Rhodophyta over 800 Ma ago. Science in China Series D: Earth Sciences, 2007, 50, 527-535.	0.9	47
102	Discussion on marine source rocks thermal evolvement patterns in the Tarim Basin and Sichuan Basin, west China. Science Bulletin, 2007, 52, 141-149.	1.7	9
103	The distribution of the oil derived from Cambrian source rocks in Lunnan area, the Tarim Basin, China. Science Bulletin, 2007, 52, 133-140.	1.7	22
104	Late Yanshan-Himalayan hydrocarbon reservoir adjustment and hydrothermal fluid activity in the central Tarim Basin. Science Bulletin, 2007, 52, 244-252.	1.7	2
105	A discussion on gas sources of the Feixianguan Formation H2S-rich giant gas fields in the northeastern Sichuan Basin. Science Bulletin, 2007, 52, 113-124.	1.7	15
106	Discussion of gas enrichment mechanism and natural gas origin in marine sedimentary basin, China. Science Bulletin, 2007, 52, 62-76.	1.7	26
107	Developmental modes of the Neoproterozoic-Lower Paleozoic marine hydrocarbon source rocks in China. Science Bulletin, 2007, 52, 77-91.	1.7	15
108	Fundamental geological elements for the occurrence of Chinese marine oil and gas accumulations. Science Bulletin, 2007, 52, 28-43.	1.7	25

SHUICHANG ZHANG

#	Article	IF	CITATIONS
109	Relations between spatial distribution and sequence types of the Cambrian-Ordovician marine source rocks in Tarim Basin. Science Bulletin, 2007, 52, 92-102.	1.7	8
110	Comments by on [Organic Geochemistry 36, 1717–1730]. Organic Geochemistry, 2006, 37, 515-518.	0.9	6
111	Kinetic modeling of individual gaseous component formed from coal in a confined system. Organic Geochemistry, 2006, 37, 932-943.	0.9	32
112	Thermal cracking history by laboratory kinetic simulation of Paleozoic oil in eastern Tarim Basin, NW China, implications for the occurrence of residual oil reservoirs. Organic Geochemistry, 2006, 37, 1803-1815.	0.9	57
113	Characteristics and quantitative of negative ion in salt aqueous solution by Raman spectroscopy at â~'170°C. Science in China Series D: Earth Sciences, 2006, 49, 124-132.	0.9	3
114	Isotopic evidence of TSR origin for natural gas bearing high H2S contents within the Feixianguan Formation of the northeastern Sichuan Basin, southwestern China. Science in China Series D: Earth Sciences, 2005, 48, 1960.	0.9	103
115	Ruthenium-ion-catalyzed oxidation of asphaltenes and oil-source correlation of heavy oils from the Lunnan and Tahe oilfields in the Tarim Basin, NW China. Diqiu Huaxue, 2005, 24, 28-36.	0.5	5
116	Geochemistry of Palaeozoic marine petroleum from the Tarim Basin, NW China: Part 1. Oil family classification. Organic Geochemistry, 2005, 36, 1204-1214.	0.9	229
117	Geochemistry of Palaeozoic marine petroleum from the Tarim Basin, NW China. Part 2: Maturity assessment. Organic Geochemistry, 2005, 36, 1215-1225.	0.9	120
118	Geochemistry and origin of sour gas accumulations in the northeastern Sichuan Basin, SW China. Organic Geochemistry, 2005, 36, 1703-1716.	0.9	95
119	Origin of the Neogene shallow gas accumulations in the Jiyang Superdepression, Bohai Bay Basin. Organic Geochemistry, 2005, 36, 1650-1663.	0.9	44
120	Geochemistry and origin of the giant Quaternary shallow gas accumulations in the eastern Qaidam Basin, NW China. Organic Geochemistry, 2005, 36, 1636-1649.	0.9	40
121	Geochemical characteristics of the Zhaolanzhuang sour gas accumulation and thermochemical sulfate reduction in the Jixian Sag of Bohai Bay Basin. Organic Geochemistry, 2005, 36, 1717-1730.	0.9	68
122	Gas systems in the Kuche Depression of the Tarim Basin: Source rock distributions, generation kinetics and gas accumulation history. Organic Geochemistry, 2005, 36, 1583-1601.	0.9	67
123	Geochemistry of petroleum systems in the eastern Pearl River Mouth Basin: evidence for mixed oils. Organic Geochemistry, 2003, 34, 971-991.	0.9	58
124	Molecular fossils and oil-source rock correlations in Tarim Basin, NW China. Science Bulletin, 2002, 47, 20-27.	1.7	67
125	The abnormal distribution of the molecular fossils in the pre-Cambrian and Cambrian: its biological significance. Science in China Series D: Earth Sciences, 2002, 45, 193-200.	0.9	85
126	Phase-controlled and gas-washing fractionations during the formation of petroleum reservoirs. Diqiu Huaxue, 2001, 20, 108-119.	0.5	1

#	Article	IF	CITATIONS
127	A kind of coccoid dinoflagellates-like fossils gives a new explanation of source of dinosterane in the Early-Middle Cambrian. Science Bulletin, 2001, 46, 420-422.	1.7	8
128	The migration fractionation: an important mechanism in the formation of condensate and waxy oil. Science Bulletin, 2000, 45, 1341-1344.	1.7	29